the plant journal

SEB SOCIETY FOR EXPERIMENTAL BIOLOGY

The Plant Journal (2025) **123,** e70335 doi: 10.1111/tpj.70335

Salicylic acid reduces ELF3 phase separation and suppresses thermomorphogenic growth in Arabidopsis

Xiangbin Chen, Ying Li, Muhammad Redzuan Bin Jamil, Jolly Madathiparambil Saju, Rajani Sarojam and Nam-Hai Chua*

Temasek Life Sciences Laboratory, 1 Research Link, National University of Singapore, Singapore 117604, Singapore

Received 11 March 2025; revised 22 June 2025; accepted 26 June 2025.
*For correspondence (e-mail chua@rockefeller.edu).

SUMMARY

Salicylic acid (SA), a long-characterized defense hormone, is increasingly recognized for its roles in plant growth and development. However, its involvement in mediating plant growth responses to environmental cues remains less understood. Here, we show that SA negatively affects thermomorphogenic growth in *Arabidopsis thaliana*. SA levels decrease in Arabidopsis when exposed to warm temperatures (29°C). Seedlings treated with exogenous SA, as well as transgenic plants with elevated SA levels, exhibit significantly reduced thermoresponsive hypocotyl elongation compared with control seedlings. By contrast, SA-deficient mutant seedlings display enhanced elongation. SA significantly decreases warmth-induced expression of *PHYTOCHROME-INTERACTING FACTOR 4* (*PIF4*), a central regulator of thermomorphogenesis, and of downstream auxin biosynthesis and signaling genes. Furthermore, the inhibitory effects of SA on thermomorphogenic growth and warmth-induced *PIF4* expression are largely dependent on *EARLY FLOWERING 3* (*ELF3*). SA reduces liquid-liquid phase separation (LLPS) of ELF3 prion-like domain (ELF3-Prd) *in vitro*, although the underlying mechanism remains to be elucidated. Correspondingly, elevated SA levels in plants decrease ELF3 nuclear speckle formation and enhance ELF3 binding to the *PIF4* promoter at warm temperatures, whereas reduced SA levels in plants lead to the opposite effect. Collectively, our study uncovers a previously unrecognized role of SA in plant growth adaptation to the changing climate.

Keywords: salicylic acid, thermomorphogenesis, warm temperature, growth, *PIF4*, ELF3, phase separation, Arabidopsis.

INTRODUCTION

For most plants, there is usually a narrow range of temperatures for their optimal growth and development. When the ambient temperature exceeds that for optimal growth, plants may experience stress and undergo a series of developmental changes to adapt to this new environment. In the case of crop plants, this growth adaptation triggered by climate disruption may comprise yield, leading to food insecurity issues (Wang et al., 2020; Zhu et al., 2022). Therefore, in the context of global climate change, it is important to understand the detailed mechanisms by which plants adapt to elevated temperatures.

In the last two decades, *Arabidopsis thaliana* has been used as a model species to uncover how ambient temperature influences plant growth-related traits (Quint et al., 2023). This model plant is usually grown under laboratory conditions at 21–22°C. In response to elevated ambient temperatures (28–29°C; warmth), Arabidopsis plants exhibit adaptive growth such as hypocotyl and petiole elongation, increased leaf hyponasty, and development of small and thin leaves. Collectively, these morphological adaptations are referred to as thermomorphogenesis (Casal & Balasubramanian, 2019; Vu et al., 2019). In general, warm temperatures affect plant growth by coordinating the activity of a network of plant hormonal signaling pathways, including those mediating responses to auxin, brassinosteroids, gibberellins, and ethylene (Gray et al., 1998; Lu et al., 2021; Stavang et al., 2009). Deciphering how elevated temperature cues are integrated with hormonal signaling is crucial for predicting and improving plant resilience under fluctuating environmental conditions.

Among the various hormonal pathways in Arabidopsis, auxin signaling plays a central role in mediating thermomorphogenic growth. Mutants deficient in auxin response or transport pathways, as well as plants containing decreased levels of free auxin, display sharply reduced thermoresponsive growth (Bellstaedt et al., 2019; Gray et al., 1998). Within the molecular framework regulating auxin pathways in Arabidopsis, the transcription factor *PHYTOCHROME-INTERACTING FACTOR 4* (*PIF4*) emerges

as a key regulator integrating elevated temperature cues to auxin-mediated plant growth (Franklin et al., 2011; Koini et al., 2009). Warm ambient temperatures promote *PIF4* transcription and increase PIF4 protein stability (Delker et al., 2022; Koini et al., 2009), which in turn activates the expression of auxin biosynthesis genes such as *YUCCA8* (*YUC8*) (Sun et al., 2012). This transcriptional activation by PIF4 leads to elevated endogenous auxin levels in plants (Franklin et al., 2011; Sun et al., 2012). Consequently, auxin accumulated in the cotyledons is transported to petioles and hypocotyl where it triggers cell elongation and thermomorphogenic growth (Bellstaedt et al., 2019).

PIF4 is known to be regulated at the transcriptional as well as post-translational level. Among the identified upstream regulators of *PIF4*, EARLY FLOWERING 3 (ELF3), a core component of the Evening Complex within the plant circadian clock, has been reported to control thermomorphogenic growth in Arabidopsis by restricting *PIF4* transcription (Box et al., 2015; Mizuno et al., 2014; Nusinow et al., 2011; Raschke et al., 2015). On the other hand, it should be noted that ELF3 can also regulate thermoresponsive flowering independently of *PIF4* (Press et al., 2016). Warm ambient temperatures are known to modulate ELF3 protein stability or activity. A recent study showed that elevated temperatures promote ELF3 protein degradation through the E3 Ubiquitin ligase XB3 ORTHOLOG 1 IN ARABIDOPSIS THALIANA (XBAT31), thereby relieving its repressive effect on *PIF4* transcription (Zhang et al., 2021). Additionally, warm temperatures trigger liquid-liquid phase separation (LLPS) of the ELF3 Prion-like domain, which further attenuates ELF3 activity (Hutin et al., 2023; Jung et al., 2020; Murcia et al., 2022). At the post-translational level, PIF4 protein is regulated by phytochrome B (phyB) which is a red and far-red photoreceptor. In its active Pfr form, phyB binds to PIF4 facilitating its degradation, whereas elevated ambient temperatures convert the photoreceptor to its inactive form (Pr) thereby releasing the PIF4 and allowing its accumulation (Jung et al., 2016).

Auxin governs plant growth and development in concert with other hormonal pathways that have been implicated in thermomorphogenesis. The defense hormone salicylic acid (SA) exhibits extensive cross talk with auxin, particularly in balancing plant growth and defense (Iglesias et al., 2011; Pasternak et al., 2019; Tan et al., 2020; Wang et al., 2007; Yuan et al., 2017). However, the role of SA in plant adaptive growth, especially in thermomorphogenic growth, remains largely unexplored. In Arabidopsis, SA is predominantly synthesized via the isochorismate pathway within chloroplasts, where isochorismate synthase (ICS) catalyzes the conversion of chorismate to isochorismate; the latter is then converted to SA by AvrPphB Susceptible 3 (PBS3) (Rekhter et al., 2019; Torrens-Spence et al., 2019; Wildermuth et al., 2001). SA can undergo various metabolic modifications, such as glucosylation forming salicylic acid glucoside (SAG) and methylation giving methyl salicylate (MeSA). These modified SA derivatives, which serve as storage or transport forms within plants, can be readily converted back to free SA to fine-tune SA homeostasis in response to environmental stimuli. In the plant defense response, SA is perceived by two groups of receptors, NON-EXPRESSER OF PR GENES 1 (NPR1) and NPR3/NPR4. SA induces defense gene expression by enhancing the transcriptional activation activity of NPR1 and suppressing the transcriptional repression activity of NPR3/NPR4 (Ding et al., 2018; Fu et al., 2012; Peng et al., 2021; Wu et al., 2012). Beyond its well-established functions in plant defense, there is increasing evidence that SA plays critical roles in regulating plant growth and development (Kaya et al., 2023; Li et al., 2022; Pokotylo et al., 2022; Rivas-San Vicente & Plasencia, 2011).

Here, we provide evidence that SA negatively affects thermomorphogenic hypocotyl growth and decreases warmth-induced expression of *PIF4* and downstream auxin pathway genes such as *YUC8* and *IAA19*. We show that *ELF3* plays a major role in mediating the inhibitory effects of SA on both the thermoresponsive *PIF4* transcription and hypocotyl elongation. SA directly reduces phase separation of ELF3 *in vitro*, although the underlying mechanism remains to be characterized. In whole plants, warm temperatures decrease SA levels, increase ELF3 nuclear speckle formation, and reduce ELF3 binding to the *PIF4* promoter. Collectively, our results uncover SA as a hitherto uncharacterized contributor to plant adaptive growth in response to elevated environmental temperatures. Our results provide new insights that may inspire future research aimed at mitigating the impacts of climate change on agriculture.

RESULTS

SA reduces thermoresponsive hypocotyl growth

Inspired by the reported extensive cross talk between SA and auxin (Iglesias et al., 2011; Pasternak et al., 2019; Tan et al., 2020; Wang et al., 2007; Yuan et al., 2017), we investigated whether SA is involved in modulating plant growth responses to elevated temperatures in Arabidopsis. We found that warm temperatures (29°C) reduced both endogenous basal SA levels (Figure 1A) and the expression of SA marker genes (Figure 1B). To further investigate the connection between endogenous SA levels and thermomorphogenesis, we employed *XVE:ICS1* plants carrying a β-estradiol inducible *ICS1*, which encodes a key enzyme for SA biosynthesis in Arabidopsis (Wildermuth et al., 2001). Plants harboring this inducible gene have been shown to significantly increase endogenous SA levels after β-estradiol induction (Ang et al., 2024). We found *XVE:ICS1* plants induced with β-estradiol and then exposed to warmth (29°C) displayed shorter hypocotyls compared

with control plants (Figure 1C,D). Similarly, wild-type (WT, Col-0) plants treated with exogenous SA and then exposed to warmth also exhibited reduced hypocotyl elongation compared with mock treatment (Figure 1E,F). The specific inhibitory effect of SA on the warmth-induced hypocotyl elongation was dependent on the SA concentration applied (Figure S1), suggesting a negative correlation between SA abundance in plants and thermoresponsive hypocotyl elongation. Notably, the SA suppressive effect on hypocotyl elongation observed at 29°C was not seen at 22°C under all the scenarios we investigated (Figure 1C–F; Figure S1).

As a volatile form of SA in plants, MeSA was shown to stimulate Arabidopsis pollen tip growth as opposed to the inhibitory effect of SA (Rong et al., 2016). To clarify the effects of SA and MeSA on the warmth-induced hypocotyl elongation, we used MeSA to fumigate WT plants before they were exposed to 29°C or kept at 22°C. Strikingly, warmth-induced hypocotyl elongation was also significantly suppressed by MeSA (Figure 1G,H), much like the effect seen with SA treatment (Figure 1E,F). It is known that MeSA has to be converted back to SA to induce pathogenesis-related (*PR*) gene *PR1* expression and trigger the plant defense response (Qi et al., 2018; Tripathi et al., 2010). Therefore, to check the true effect of MeSA on thermomorphogenic hypocotyl growth, we employed a specific inhibitor of MeSA esterases, 2,2,2,2′-Tetrafluoroacetophenone (TetraFA) (Park et al., 2009), to block the conversion of MeSA to SA in plants fumigated with MeSA. As expected, MeSA-induced *PR1* expression was almost completely blocked when plants were incubated with TetraFA (Figure S2), confirming its inhibitory effect on MeSA esterase. Using the same inhibitor TetraFA, we found that the inhibitory effect of MeSA on warm temperature-induced hypocotyl elongation was completely erased when the conversion of MeSA to SA was prevented (Figure 1G–I). This result suggests that MeSA has to be converted back to SA to modulate thermomorphogenic hypocotyl growth. Thus, SA but not MeSA acts as the active form to decrease hypocotyl elongation in response to warmth.

In contrast to the inducer-treated *XVE:ICS1* plants, the *ics1* mutant, which is deficient in SA biosynthesis, displayed slightly but significantly enhanced hypocotyl growth compared with WT plants at warm temperatures (Figure 1J,K). Moreover, this hypocotyl elongation phenotype of *ics1* was reverted to WT-like phenotype by exogenous application of SA (Figure S3). These results suggest the altered responsiveness of *ics1* to elevated temperature is due to the deficiency in SA biosynthesis. Consistent with the results obtained with *XVE:ICS1* and exogenous SA application (Figure 1C–F), hypocotyl elongation was not significantly changed in the *ics1* mutant compared with WT at 22°C (Figure 1J,K). As the warmth-induced hypocotyl elongation is a widely recognized characteristic phenotype for thermomorphogenesis (Casal & Balasubramanian, 2019; Delker et al., 2022), our results provide evidence that SA is a significant player regulating thermomorphogenic growth in Arabidopsis.

SA decreases warm temperature-induced *PIF4* expression

Previous studies have established that *PIF4* is a major positive regulator of thermomorphogenesis and its expression is induced by elevated ambient temperatures at multiple levels ranging from transcriptional activation to protein stability (Delker et al., 2022; Koini et al., 2009). It was also reported that *PIF4* promoter activity largely accounts for the temperature-dependent changes in PIF4 protein levels (Murcia et al., 2022). Because we found SA negatively affects hypocotyl thermomorphogenic growth in Arabidopsis (Figure 1), we further investigated the effects of SA on warmth-induced *PIF4* expression. As methylation confers SA better membrane permeability in plants (Huang et al., 2020), we used MeSA fumigation here to more robustly characterize the effect of SA on thermoresponsive gene expression. *pPIF4:GUS* plants were used to monitor the responsiveness of *PIF4* promoter activity to changes in ambient temperatures. We found increased GUS expression in cotyledon cells of mock control plants after 2 h of warm temperature treatment (Figure 2A); by contrast, GUS expression was markedly reduced in the cotyledon cells of MeSA-fumigated plants compared with mock controls under the same temperature treatment (Figure 2A). The GUS staining results were confirmed by transcript analysis by RT-qPCR. *PIF4* transcript levels in WT plants at warm temperatures were significantly reduced by MeSA fumigation (Figure 2B). Along with the altered *PIF4* expression, the expression of downstream auxin pathway genes, such as *YUC8* and *INDOLE-3-ACETIC ACID INDUCIBLE 19* (*IAA19*) was also significantly reduced by MeSA fumigation (Figure 2B), reflecting the effects of decreased *PIF4* promoter activity due to SA.

Next, we asked whether changes in endogenous SA levels would also affect warmth-induced expression of *PIF4* and its downstream genes. We found that the expression of *PIF4* and its downstream auxin-related genes in β-estradiol-treated *XVE:ICS1* plants was lower compared with *XVE:NC* control plants at 29°C (Figure 2C). By contrast, the induction of the expression of these thermoresponsive genes was higher in *ics1* mutant compared with WT plants at the same temperature treatment (Figure 2D). Control experiments showed that the expression of *PIF4* and its downstream genes at normal temperatures (22°C) was not changed by SA treatment nor affected by endogenous SA levels (Figure 2). Taken together, these results show that SA decreases warmth-induced expression of *PIF4* and its downstream genes.

ELF3 plays a major role in mediating the effect of SA on thermomorphogenic growth

To further explore the mode of SA action in thermomorphogenesis, we investigated the requirement of *PIF4* in this process. We found that the inhibition of hypocotyl elongation by SA was pronouncedly reduced in *pif4* compared with WT at 29°C (4.2% vs. 23.9%) (Figure 3A,B). This result suggests *PIF4* plays a dominant role in the effect of SA on thermomorphogenic growth. Although both ELF3 and phyB are known regulators of thermomorphogenesis, they act on *PIF4* at different levels. ELF3 is a component of the Evening Complex that functions as a transcriptional repressor, and it governs temperature-dependent regulation of *PIF4* expression (Box et al., 2015; Ezer et al., 2017; Mizuno et al., 2014; Raschke et al., 2015). By contrast, phyB negatively regulates PIF4 protein stability (Lorrain et al., 2008). We found the sensitivity of hypocotyl elongation to SA treatment at 29°C in *elf3* was markedly decreased compared with WT (5.4% vs. 23.9%), whereas the sensitivity of the *phyB* mutant to SA treatment was comparable to that

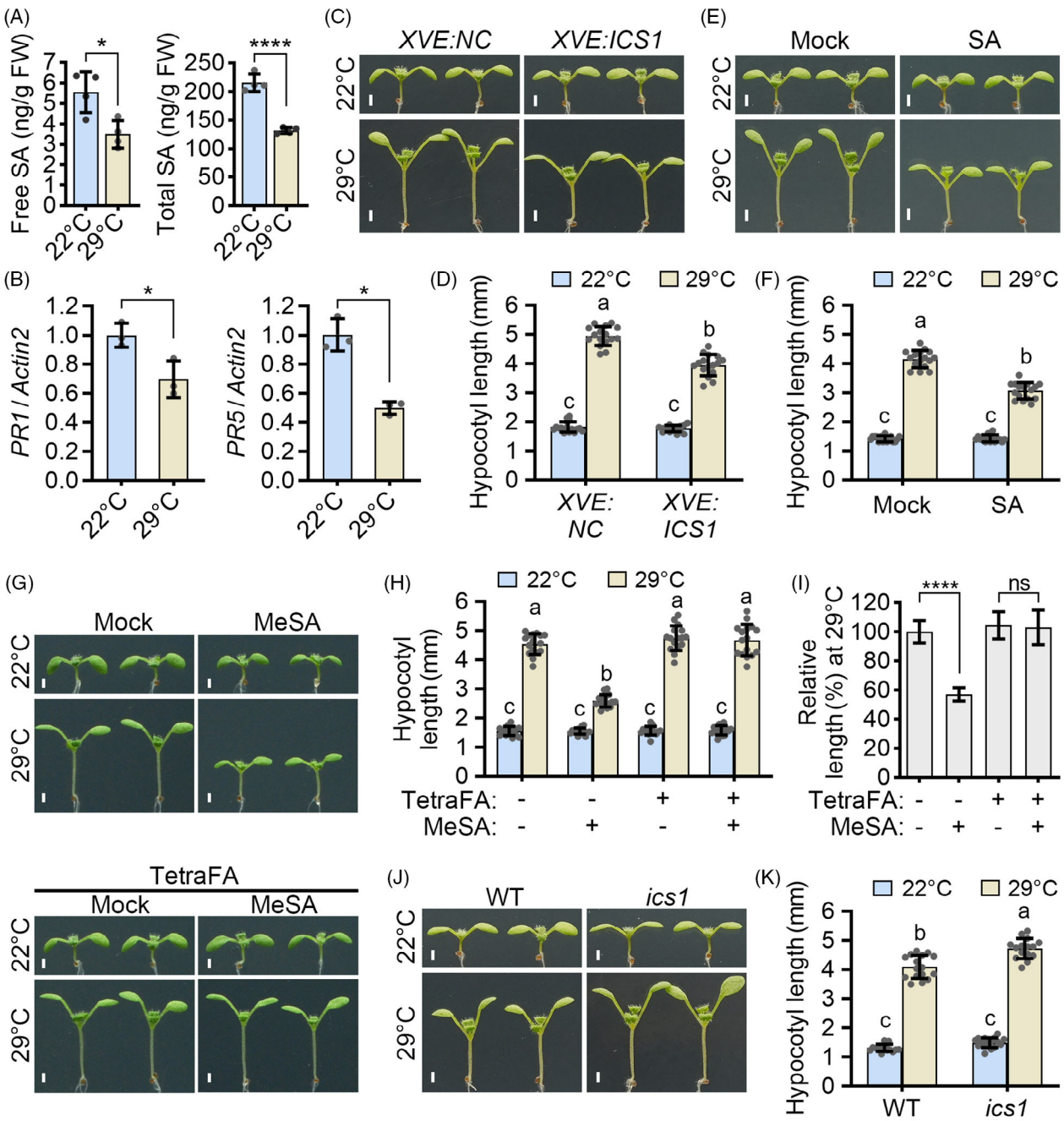

Figure 1. SA suppresses thermoresponsive hypocotyl growth in Arabidopsis.
(A) SA levels in WT plants grown at normal or high ambient temperature. WT seedlings were grown at 22°C for 5 days and then either kept at 22°C or transferred to 29°C for an additional 24 h before sampling for quantification of SA. Data are mean ± SD, $n = 4$ biological replicates. More than 100 seedlings were included in each biological replicate. Student's *t*-test, $^{*}P < 0.05$; $^{****}P < 0.0001$.
(B) Effects of warm temperatures on *PR1* and *PR5* expression. WT seedlings were grown at 22°C for 4 days and then either kept at 22°C or transferred to 29°C for another 6 h before gene expression was examined. Data are mean ± SD, $n = 3$ biological replicates. Student's *t*-test, $^{*}P < 0.05$.
(C, D) Phenotypes of *ICS1*-overexpression plants at normal or high ambient temperature. *XVE:ICS1* and *XVE:NC* seedlings were grown at 22°C for 4 days, transferred to medium supplemented with 10 μM β-estradiol for an additional 24 h, and then either kept at 22°C or transferred to 29°C for another 4 days. Representative plants were imaged (C) and the hypocotyl length was measured (D).
(E, F) Phenotypes of SA treated WT plants at normal or high ambient temperature. WT seedlings were grown at 22°C for 4 days, transferred to medium with or without 20 μM SA for an additional 4 h, and then either kept at 22°C or transferred to 29°C for another 4 days. Representative plants were imaged (E) and the hypocotyl length was measured (F).
(G–I) Inactivation of MeSA esterase blocks the inhibitory effect of MeSA on thermomorphogenesis. WT seedlings were grown at 22°C for 4 days, transferred to medium supplemented with or without 50 μM TetraFA for an additional 24 h, and then fumigated with or without 15 μM MeSA for 4 h. Plants were then either kept at 22°C or transferred to 29°C for another 4 days. Representative plants were imaged (G), the hypocotyl length was measured (H) and the relative hypocotyl length of seedlings compared with control seedlings at 29°C was calculated (I). Student's *t*-test, $^{****}P < 0.0001$; ns, not significant.
(J, K) Phenotypes of *ics1* mutant plants at normal or high ambient temperature. WT and *ics1* mutant seedlings were grown at 22°C for 4 days, and then either kept at 22°C or transferred to 29°C for another 4 days. Representative plants were imaged (J) and the hypocotyl length was measured (K).
(C–H, J, K) Scale bar, 1 mm. $n = 15$–16 seedlings. Data are mean ± SD. Different letters represent significant differences with $P < 0.05$, by Tukey's test following one-way analysis of variance (ANOVA).

of WT (22.0% vs. 23.9%) (Figure 3A,B). These results suggest that *ELF3*, rather than *phyB*, plays a major role in mediating the inhibitory effect of SA on thermomorphogenic growth. Consistent with this notion, cycloheximide (CHX) chase experiments showed the degradation rate of PIF4 protein in plants treated with SA was similar to that in mock-treated plants, suggesting that SA has minimal effect on PIF4 protein stability at 29°C (Figure S4).

We investigated whether any of the three well-established SA receptors NPR1, NPR3, and NPR4 in Arabidopsis (Fu et al., 2012; Wu et al., 2012) are involved in the effect of SA on thermomorphogenesis. To this end, we examined the effects of SA on thermoresponsive hypocotyl elongation of the *npr1/3/4* triple mutant. Unexpectedly, *npr1/3/4* mutant hypocotyl elongation at 29°C still displayed pronounced sensitivity (20.0%) to SA treatment, which is close to the sensitivity observed in WT (22.9%) (Figure 3C,D). This result led us to conclude that the three SA receptors play a limited role in mediating the effect of SA on thermomorphogenic hypocotyl growth.

SA reduces ELF3 phase separation and promotes ELF3 binding to the *PIF4* promoter

Consistent with the critical role of *ELF3* in the inhibitory effect of SA on thermomorphogenic growth, we found the suppressive effect of SA on *PIF4* expression at 29°C observed in the WT was completely abolished in *elf3* (Figure 4A). This result suggests that the suppression of *PIF4* expression by SA at 29°C also depends on *ELF3*. To explore how SA modulates ELF3 to suppress *PIF4* expression at warm ambient temperatures, we introduced *pELF3:ELF3-mGFP* into plants of different genotypes: WT, *ics1*, *XVE:ICS1*, and control *XVE:NC*. Plants expressing comparable levels of *ELF3-mGFP* mRNA in β-estradiol treated *XVE:ICS1* and control *XVE:NC* plants were used to check for ELF3-mGFP protein expression. We found that ELF3-mGFP protein levels were not changed by inducible overexpression of *ICS1* in plants (Figure 4B; Figure S5A,B). Similar ELF3-mGFP protein levels were also observed in the *ics1* mutant compared with WT (Figure 4C; Figure S5C,D). These results suggest that SA has little effect on ELF3 protein stability in Arabidopsis.

Next, we tested the effect of SA on ELF3 binding to the *PIF4* promoter by chromatin immunoprecipitation. We found that the level of ELF3-mGFP enrichment on the *PIF4* promoter was higher in β-estradiol-treated *XVE:ICS1* plants compared with *XVE:NC* control plants at 29°C (Figure 4D). Conversely, the level of ELF3-mGFP enrichment was lower in *ics1* compared with WT at the same temperature (Figure 4E). These results suggest that SA promotes ELF3 association with the *PIF4* promoter, thereby repressing *PIF4* expression at warm temperatures. ELF3 has been reported to undergo reversible phase separation driven by its prion-like domain (Prd) and this protein forms nuclear speckles, transitioning from an active to an inactive state in response to elevated temperatures (Hutin et al., 2023; Jung et al., 2020; Murcia et al., 2022). Given our finding that SA promotes ELF3 chromatin binding at 29°C (Figure 4D,E), we investigated whether SA affects ELF3 phase separation, which is related to the partitioning of ELF3 in nuclear speckles or its becoming chromatin-bound (Jung et al., 2020; Murcia et al., 2022). We confirmed the previous finding that purified recombinant ELF3-Prd was able to undergo LLPS *in vitro* (Figure S6) (Hutin et al., 2023; Jung et al., 2020). Notably, the number of ELF3-Prd LLPS droplets formed *in vitro* was markedly reduced by the addition of SA (Figure 4F), indicating SA inhibits ELF3 phase separation. However, the mechanism of this inhibition remains to be investigated in future experiments. To explore if the SA inhibitory effects on the phase separation of LLPS can be seen *in vivo*, we examined the effects of different SA levels on the formation of ELF3 nuclear speckles in Arabidopsis at warm temperatures. The number of ELF3-mGFP

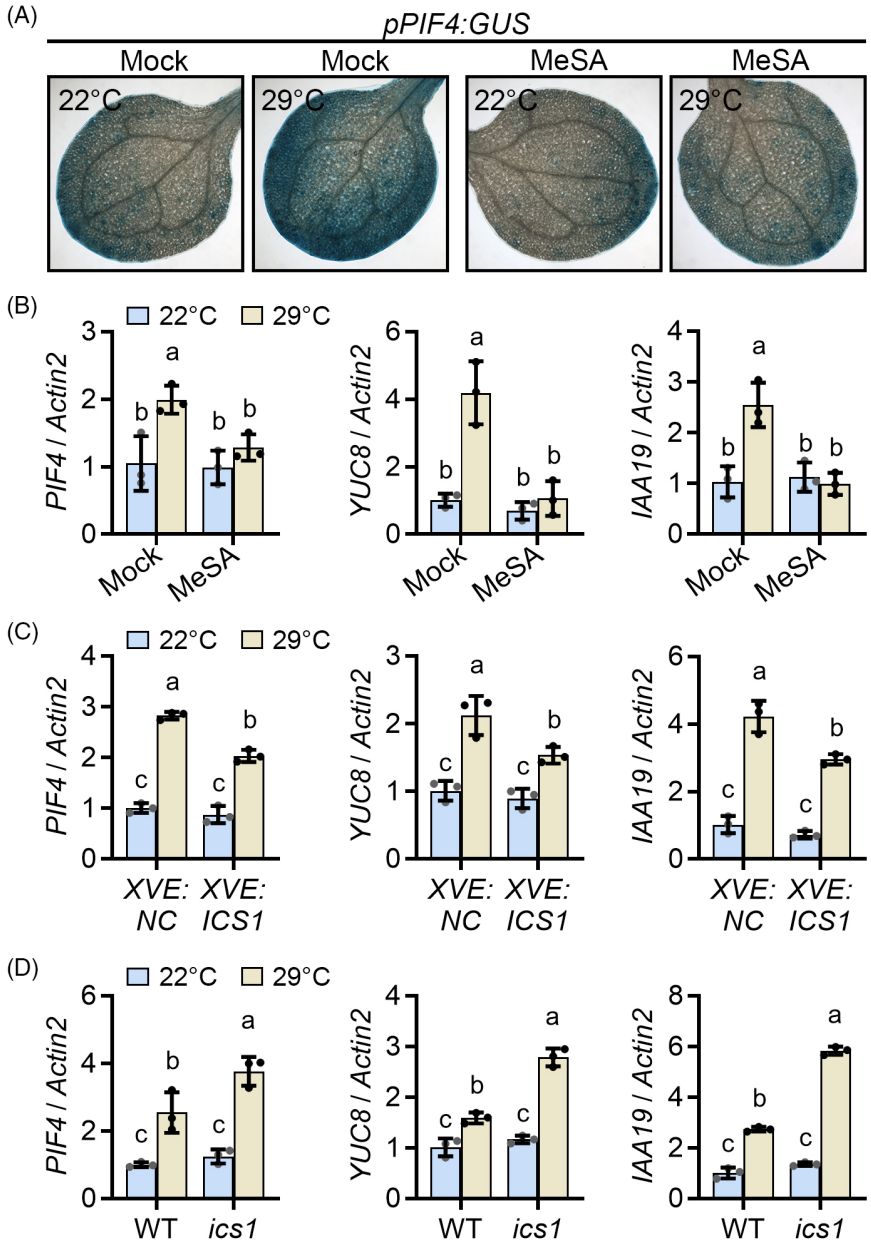

Figure 2. SA decreases warmth-induced expression of *PIF4* and its downstream target genes.
(A) Effects of SA on thermoresponsive *PIF4* promoter activity. *pPIF4:GUS* seedlings were grown at 22°C for 6 days, fumigated with or without 15 μM MeSA for 4 h, and then kept at 22°C or moved to 29°C for 2 h. Plants were then sampled for GUS staining.
(B) Relative expression of *PIF4* and its target genes *YUC8* and *IAA19* in SA treated WT plants in response to elevated temperatures. WT seedlings were grown at 22°C for 6 days, fumigated with or without 15 μM MeSA for 4 h, and then kept at 22°C or moved to 29°C for 4 h. Cotyledons of each plant were harvested and total RNA was extracted for gene expression analysis.
(C) Relative expression of *PIF4* and its target genes *YUC8* and *IAA19* in *ICS1*-overexpression plants in response to elevated temperatures. *XVE:ICS1* and *XVE:NC* seedlings were grown at 22°C for 6 days, transferred to medium supplemented with 10 μM β-estradiol for an additional 24 h, and then kept at 22°C or moved to 29°C for 4 h. Whole seedlings were analyzed for gene expression.
(D) Relative expression of *PIF4* and its target genes *YUC8* and *IAA19* in *ics1* mutant plants in response to elevated temperatures. WT and *ics1* mutant seedlings were grown at 22°C for 6 days and then kept at 22°C or moved to 29°C for 4 h. Whole seedlings were analyzed for gene expression.
(B–D) Data are mean ± SD. $n = 3$ biological replicates. Different letters represent significant differences with $P < 0.05$, by Tukey's test following one-way ANOVA.

nuclear speckles in β-estradiol-treated *XVE:ICS1* plants was decreased compared with *XVE:NC* control plants (Figure 4G,I); by contrast, the number of ELF3-mGFP nuclear speckles in *ics1* was increased compared with WT (Figure 4H,J). ELF3 speckle formation and chromatin binding activity have been shown to be negatively correlated

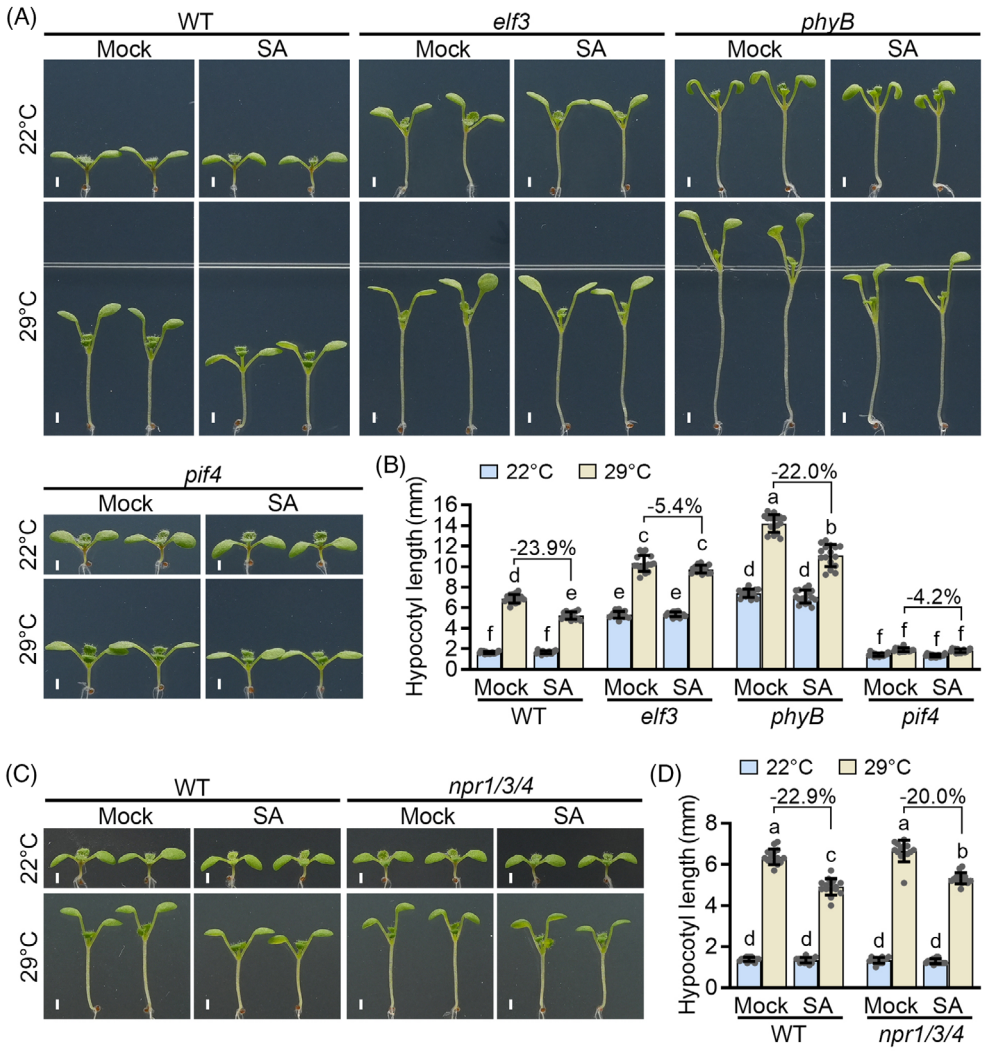

Figure 3. The effect of SA on thermoresponsive hypocotyl growth is impaired in *elf3* mutants.
(A, B) The effect of *elf3*, *phyB*, or *pif4* mutation on the sensitivity of thermoresponsive hypocotyl elongation to SA treatment. WT, *elf3*, *phyB*, and *pif4* mutant seedlings were grown at 22°C for 4 days, transferred to medium with or without 20 μM SA for an additional 4 h, and then either kept at 22°C or transferred to 29°C for another 4 days. Representative plants were imaged (A) and the hypocotyl length was measured (B).
(C, D) The effect of *npr1*, *npr3*, and *npr4* triple mutations on the sensitivity of thermoresponsive hypocotyl elongation to SA treatment. WT and *npr1/3/4* triple mutant seedlings were grown at 22°C for 4 days, transferred to medium with or without 20 μM SA for an additional 4 h, and then either kept at 22°C or transferred to 29°C for another 4 days. Representative plants were imaged (C) and the hypocotyl length was measured (D).
(A–D) Scale bar, 1 mm. n = 13–16 seedlings. Data are mean ± SD. Different letters represent significant differences with $P < 0.05$, by Tukey's test following one-way ANOVA.

(Jung et al., 2020, Murcia et al., 2022). Our findings that SA reduces ELF3 phase separation and that SA promotes ELF3 binding to the *PIF4* promoter are consistent with the negative correlation observed previously (Figure 4D–J). Together, our results explain the inhibitory effect of SA on thermomorphogenic growth in Arabidopsis.

DISCUSSION

When challenged with elevated ambient temperatures, plants implement growth adaptation by elongating their organs to increase their cooling capacity. This thermomorphogenic growth is mediated by an integration of temperature cues and signaling of plant hormones (Lu et al., 2021; Quint et al., 2023). Although auxin and other plant hormones have been implicated in plant thermomorphogenesis (Lu et al., 2021), our understanding of the involvement of hormones and their interactions in plant thermomorphogenic growth remains incomplete. Here, we show that SA, a long-characterized defense hormone, restricts warmth-induced expression of auxin biosynthesis and signaling genes and suppresses thermomorphogenic hypocotyl growth in Arabidopsis.

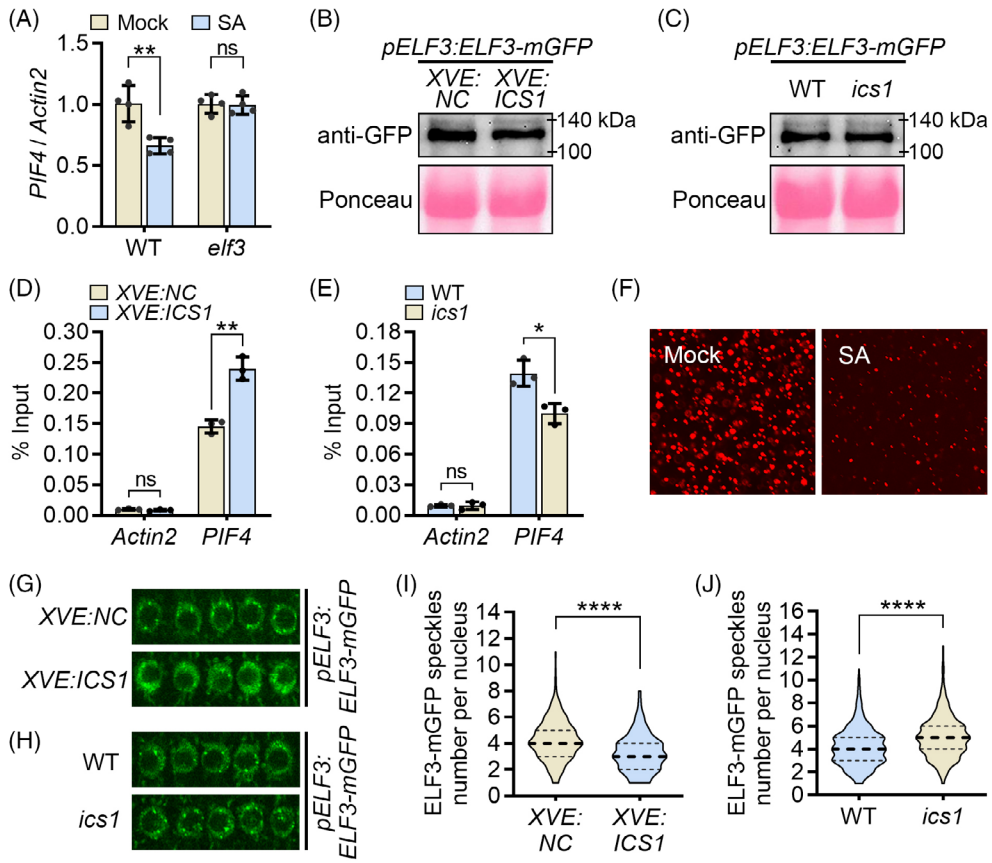

Figure 4. SA reduces ELF3 phase separation and enhances ELF3 binding to *PIF4* promoter.
(A) Relative expression of *PIF4* in WT and *elf3* mutants with or without SA treatment at warm ambient temperature. WT and *elf3* mutant seedlings were grown at 22°C for 6 days, transferred to medium with or without 20 μM SA for an additional 2 h, and then transferred to 29°C for 4 h. Whole seedlings were sampled for gene expression analysis. Student's *t*-test, $^{**}P < 0.01$; ns, not significant.
(B, D) Immunoblot analysis for the ELF3-mGFP protein levels and ChIP analysis of enrichment of ELF3-mGFP on the *PIF4* promoter in *ICS1*-overexpression plants at warm temperature. *pELF3:ELF3-mGFP* in *XVE:ICS1* and *pELF3:ELF3-mGFP* in *XVE:NC* seedlings were grown at 22°C for 6 days, transferred to medium supplemented with 10 μM β-estradiol for an additional 24 h, and then moved to 29°C for 3 h. Whole seedlings were sampled for immunoblot (B) and ChIP (D) analysis. Student's *t*-test, $^{**}P < 0.01$; ns, not significant.
(C, E) Immunoblot analysis for the ELF3-mGFP protein levels and ChIP analysis of enrichment of ELF3-mGFP on the PIF4 promoter in *ics1* mutant plants at warm temperature. *pELF3:ELF3-mGFP* in WT and *pELF3:ELF3-mGFP* in *ics1* mutant seedlings were grown at 22°C for 6 days and then moved to 29°C for 3 h. Whole seedlings were sampled for immunoblot (C) and ChIP (E) analysis. Student's *t*-test, $^{*}P < 0.05$; ns, not significant.
(F) Effect of SA on LLPS formation of MBP-ELF3-Prd-mCherry protein *in vitro*.
(G, I) ELF3-mGFP nuclear speckles in *ICS1*-overexpression plants at warm temperature. *pELF3:ELF3-mGFP* in *XVE:ICS1* and pELF3:ELF3-mGFP in *XVE:NC* seedlings were grown at 22°C for 6 days, transferred to medium supplemented with 10 μM β-estradiol for an additional 24 h, and then moved to 29°C for 3 h. Representative ELF3-mGFP nuclear speckles were imaged (G) and the number of ELF3-mGFP nuclear speckles was quantified (I). Student's *t*-test, $^{****}P < 0.0001$.
(H, J) ELF3-mGFP nuclear speckles in *ics1* mutant plants at warm temperature. *pELF3:ELF3-mGFP* in WT and *pELF3:ELF3-mGFP* in *ics1* mutant seedlings were grown at 22°C for 6 days and then moved to 29°C for 3 h. Representative ELF3-mGFP nuclear speckles were imaged (H) and the number of ELF3-mGFP nuclear speckles was quantified (J). Student's *t*-test, $^{****}P < 0.0001$.

Previous studies have characterized the cross talk between SA and auxin, especially the effects of SA on auxin biosynthesis, homeostasis, transport, and signaling (Iglesias et al., 2011; Pasternak et al., 2019; Tan et al., 2020; Yuan et al., 2017; Zhang et al., 2007). These studies reveal that SA, beyond its defense function, also restricts the growth-promoting functions of auxin through distinct regulatory mechanisms. Our finding that SA suppresses auxin pathway genes and thermomorphogenic hypocotyl growth further supports the antagonistic roles of SA and auxin in plant growth, particularly during adaptation to elevated ambient temperatures. Consistent with this, we observed that SA levels were lower in Arabidopsis transferred to warm temperatures (29°C) compared with those maintained at normal temperatures (22°C) (Figure 1A). This suggests a likely adaptive reduction of SA levels in response to elevated temperatures, although the underlying mechanism remains unknown. By contrast, the suppression of SA production in pathogen-infected Arabidopsis under high-temperature conditions has been elucidated (Kim et al., 2022). Nevertheless, a recent study reported that even in the absence of active defense responses, healthy

Arabidopsis plants still require adequate basal levels of SA to enable early pathogen detection and prompt immune activation (van Butselaar et al., 2024). Therefore, considering the phenomenon of promoting growth at the expense of defense capacity, we speculate that the reduction of SA levels in non-infected Arabidopsis may serve to alleviate its inhibitory effect on auxin biosynthesis and signaling, thereby facilitating thermomorphogenic growth in plants.

Our results show that *ELF3* plays a major role in mediating the effect of SA on thermomorphogenic growth and *PIF4* expression at warm temperatures (Figures 3 and 4A). However, we note that the sensitivity of thermoresponsive hypocotyl elongation to SA was not completely abolished in *elf3* (Figure 3A,B), leaving open the possible involvement of additional signaling pathways. Previous studies have shown that auxin redistribution, mediated by polar auxin transport, connects temperature sensing in the cotyledons with thermoresponsive elongation of the hypocotyl in Arabidopsis (Bellstaedt et al., 2019). Moreover, SA has been shown to affect polar auxin transport in regulating root gravitropism and growth (Ke et al., 2021; Tan et al., 2020). Therefore, whether auxin transport is involved in the effect of SA on thermomorphogenic growth remains to be elucidated.

Increasing evidence shows that SA can suppress plant growth without the participation of NPR1, 3, and 4 receptor proteins (Jia et al., 2025; Rong et al., 2016; Tan et al., 2020). On the other hand, the three NPR proteins can also have SA-independent functions (Lai et al., 2018; Olate et al., 2018). Here, we found SA negatively affects hypocotyl thermoresponsive growth in a manner independent of NPR1/3/4 proteins in Arabidopsis (Figure 3C,D). Beyond the well-established NPR proteins, numerous SA-binding proteins (SABPs) have been identified. These SABPs bind SA with varying affinities and play diverse roles in cellular regulation in plants (Manohar et al., 2014; Pokotylo et al., 2019). Against this background, we cannot rule out the possibility that one or more SABPs may mediate the effects of SA on thermomorphogenic growth. Although our data demonstrate that SA can directly reduce ELF3 phase separation *in vitro* (Figure 4F), which correlates with the effect of SA on hypocotyl growth, the potential involvement of SABPs in the effect of SA *in vivo* cannot be excluded.

In Arabidopsis, ELF3 contains a prion-like domain with polyglutamine (polyQ) tracts. The length of the polyQ tract varies across natural accessions of *A. thaliana* (Undurraga et al., 2012). Recent studies have shown that ELF3 undergoes phase separation to form nuclear speckles in a temperature-sensitive manner, and this process is driven by its prion-like domain (Hutin et al., 2023; Jung et al., 2020). Variations in polyQ length tune the onset and range of LLPS and affect the propensity of ELF3 to form speckles (Hutin et al., 2023, Jung et al., 2020). However, the effect of the ELF3-polyQ tract length on thermal responses in plants remains controversial (Jung et al., 2020; Press et al., 2016; Undurraga et al., 2012; Zhu et al., 2024). Nevertheless, ELF3 speckle formation has been shown to be associated with reduced ELF3 activity, as supported by the strong positive correlation between the number of ELF3 nuclear speckles and *PIF4* promoter activity (Murcia et al., 2022). We found that SA inhibits ELF3 phase separation *in vitro* (Figure 4F), suggesting the effect of SA is direct and SA shifts the equilibrium toward free ELF3. In plants, elevated and reduced SA levels lead to decreased and increased numbers of ELF3 nuclear speckles, respectively. These results are consistent with the results obtained *in vitro*. We found that the effect of SA on the number of ELF3-containing speckles is inversely correlated with its effect on ELF3 occupancy at the *PIF4* promoter, aligning with previous findings regarding the relationship between ELF3 speckle formation and *PIF4* promoter activity in Arabidopsis (Murcia et al., 2022). Elevated SA levels yield fewer speckles and more binding of ELF3 to the *PIF4* promoter, whereas reduced SA levels result in more ELF3 speckles and diminished promoter binding (Figure 4D–J). Based on this correlation, we assume that the reduction of ELF3 phase separation by SA and the increase of ELF3 binding to the *PIF4* promoter by SA is likely related. The effects of SA on ELF3 activity support our findings that SA negatively affects thermoresponsive gene expression and thermomorphogenic growth in Arabidopsis.

Although our *in vitro* experiments show that the effect of SA on ELF3-Prd phase separation is direct, the mechanism of the SA-mediated inhibition remains to be characterized. Recent studies showed that a decrease in pH favors the phase separation of ELF3-Prd (Hutin et al., 2023, Jung et al., 2020). As a weak acid, SA has been reported to lower the intracellular pH (Emoto et al., 2002). Therefore, the inhibition of ELF3 phase separation by SA is unlikely to result from pH changes. A recent review suggested that small molecules may bind to and modify intramolecular interactions of proteins that enable phase separation (Maruri-Lopez & Chodasiewicz, 2023). Thus, it would be worthwhile to investigate whether SA directly binds to the ELF3 protein in future studies.

Taken together, our results uncover a previously unrecognized role of SA in plant adaptive growth in response to elevated temperatures. We propose that adequate SA levels in plants are required to maintain a reduced number of ELF3 nuclear speckles, increase ELF3 binding to the *PIF4* promoter, and lower expression of *PIF4* and auxin pathway genes. Under these conditions, plant growth is regulated and its defense capacity is preserved. Warm temperatures lower SA levels, relieving its effect on the ELF3-*PIF4*-auxin pathway and facilitating thermomorphogenic growth. In light of global warming trends and the well-established role of SA in plant defense, our

identification of its involvement in regulating thermomorphogenic growth provides new insights into improving plant resilience under climate change.

MATERIALS AND METHODS

Plant materials and growth conditions

All *A. thaliana* plants used in this study are Columbia (Col) ecotype. The Col-0 (CS70000) from Arabidopsis Biological Resource Center (ABRC) was used as the wild-type (WT). Seeds of *ics1* (SALK_111380C), *elf3* (SALK_202881C), *phyB* (CS71625), *pif4* (CS66043) mutants, and *pPIF4:GUS* (CS69169) were obtained from ABRC. The *npr1/3/4* triple mutant was generated in this study by genetic crossing of *npr1* (SALK_204100C) and *npr3/4* (CS72351). All T-DNA insertion mutants used were genotyped using the primers from T-DNA Primer Designed Tool (http://signal.salk.edu/tdnaprimers.2.html) (Table S1). The generation of *XVE:ICS1* plants was previously described (Ang et al., 2024). The empty *XVE* vector (*pER8*) (Zuo et al., 2000) without any inserted coding sequence was designated *XVE:NC* and used as a negative control. To generate the *pELF3:ELF3-mGFP* construct, coding sequences of monomeric GFP and ELF3 were respectively amplified and sequentially subcloned into *pCaMV35S: OCS* vector to generate the *pCaMV35S: ELF3-mGFP* expression cassette. A 3.5 kb genomic fragment upstream from the translation start codon of *ELF3* was further subcloned into the vector. Vectors were transformed into Arabidopsis plants using the floral dipping method (Zhang et al., 2006). Transgenic plants were isolated by antibiotic selection and propagated to obtain single insertion homozygous lines.

Arabidopsis seeds were surface sterilized and spread on medium containing 2.2 g L^{-1} Murashige & Skoog medium (Duchefa), 0.5 g L^{-1} MES, 1% sucrose, pH = 5.8 adjusted by KOH, and 0.8% agar. Sterilized seeds were then stratified at 4°C in the dark for 3 days, followed by germination and treatment under long-day photoperiod (16 h light and 8 h dark) at light intensity of 85 μmol m^{-2} $sec,^{-1}$ with specific temperature conditions in plant growth chambers (Percival Scientific). Images of seedlings were taken with a digital camera, and the hypocotyl length of each plant was measured using ImageJ software (https://imagej.net/ij/).

Metabolite extraction and analysis

Approximately, 150 mg of weighed whole seedlings were homogenized into a fine powder in liquid nitrogen and subsequently extracted in 1 mL of 80% (v/v) methanol at 4°C for 2 h with gentle rotation. After centrifugation at 13 000×***g*** for 10 min at 4°C, the supernatant was collected and filtered by Costar® Spin-X® centrifuge tube with 0.22 μm pore nylon membrane (Corning, # 8169). About 200 μL of the filtered extraction was used to measure the contents of free SA. For total SA (sum of free SA and SA glucosides), the extract was hydrolyzed with β-glucosidase according to the protocol previously described (Zhang et al., 2017) with minor modifications to release free SA for measurement. Briefly, another 200 μL of the filtered extract was dried using a Concentrator plus complete system (Eppendorf, #5305000762) and the pellet was dissolved in 100 μL of 100 mM sodium acetate (pH = 5.5) and treated with 100 μL of 20 U mL^{-1} β-glucosidase (Sigma, # 49290) at 37°C for 2 h. Then, the hydrolyzed samples were incubated at 100°C for 5 min and centrifuged at 13 000×***g*** for 10 min at 4°C to collect the supernatant. For SA quantification, samples were analyzed using Agilent 6495 triple quadrupole liquid chromatography-mass spectrometry (LC–MS) system. The chromatographic separation was carried out by Thermo Scientific™ Accucore™ RP-MS HPLC Column (2.1 × 100 mm, 2.6 μm) (Fisher Scientific, #11337531) operating at 35°C. The mobile phase was comprised of 0.5% formic acid (A) and 100% methanol (B), respectively. The flow rate was 300 μL min^{-1}, and the program of gradient elution was as follows: 0–1 min, 30% B; 1–11 min, 30–55% B; 11–13 min, 55–100% B; 13–15 min, 100% B; 15–16 min, 100%–30% B; 16–17 min, 30% B. The injection volume of each sample was 2 μL. Eluted samples were introduced into Agilent Jet Stream Electrospray Ionization (AJS-ESI) ion source and conducted in negative ion mode. Multiple reaction monitoring (MRM) mode was used to monitor specific precursor ions → product ions transitions for SA (*m/z* 137.02 → 93.1, and 137.02 → 65.2). The product ions at *m/z* 93.1 were selected as quantifier ions, whereas product ions at *m/z* 65.2 were selected as qualifier ions during data processing. SA (Sigma, PHR1013) was dissolved in solvent, and a solution of varying concentrations was generated by serial dilution. Different SA concentrations were measured to generate a standard curve, which was used to calculate the concentrations of SA in samples.

Chemicals treatment

For SA or TetraFA treatment, Arabidopsis seedlings at the specified age were transferred to fresh medium supplemented with the respective compound at the target concentration or to control medium without the compound, and incubated under the indicated experimental conditions.

For MeSA fumigation, a sterilized flat cap of PCR tube was placed on the surface of the MS medium at the center of a horizontally positioned Petri dish containing Arabidopsis seedlings. The required volume of MeSA, calculated based on the internal airspace (i.e., the air volume within the Petri dish) to achieve the desired concentration, was applied to the center of the cap. The dish was then sealed with airtight tape and incubated under the designated conditions.

RNA extraction and transcript analysis

Total RNA from seedlings was extracted and purified with EasyPure® Plant RNA Kit (TransGen Biotech, ER301). About 1 μg of total RNA was reverse transcribed using iScript™ cDNA Synthesis Kit (Bio-Rad, #1708891). qPCR reactions including diluted cDNA, gene-specific primers, and SsoAdvanced Universal SYBR® Green Supermix (Bio-Rad, #1725274) were performed in 96-well blocks with the CFX Connect Real-Time PCR Detection System (Bio-Rad). Relative gene expression was analyzed using the $2^{(-\Delta\Delta CT)}$ method. The sequences of relevant primers are listed in Table S1.

Cycloheximide (CHX) chase assay

Arabidopsis seedlings overexpressing *PIF4-HA* at 6 dpg growing at 22°C were treated with 4 h of DMSO or 20 μM SA. The plants were then shifted to 29°C for 4 h. Following this, the seedlings were shifted to medium supplemented with 200 μM CHX. Samples were collected at the starting point and at 15-min intervals thereafter for immunoblot analysis of PIF4-HA protein levels.

Immunoblotting

Total protein from seedlings was extracted in NuPAGE™ LDS sample buffer (Thermo Fisher Scientific, NP0008) with 50 μL mL^{-1} 2-mercaptoethanol. Samples were boiled for 10 min and centrifuged at 20 000×***g*** for 10 min. Supernatant was collected and separated on a 10% SDS-PAGE gel and transferred onto an Immobilon®-P PVDF Membrane (Merck Millipore, IPVH00010). Membrane was blocked in 5% non-fat dry milk (Santa Cruz Biotechnology,

sc-2324) in TBST buffer (25 mM Tris, pH8.0, 150 mM NaCl, 0.1% Tween-20) at room temperature for 1 h and then incubated with a 1:3000 dilution of GFP Antibody (B-2) (Santa Cruz Biotechnology, sc-9996) at 4°C overnight. After three times of 10-min washes with TBST buffer, the membrane was incubated with a 1:5000 dilution of ECL Anti-Mouse IgG, horseradish peroxidase-linked whole antibody (from sheep) secondary antibody (Cytiva, NA931) at room temperature for 1 h. After three times of 10 min washes with TBST buffer, the signals were detected using Clarity Max Western ECL Substrate (Bio-Rad, #1705062) via an iBright imaging system (Invitrogen).

Chromatin immunoprecipitation (ChIP) assay

Approximately, 1 g of whole seedlings were cross-linked by 1% formaldehyde, and the reaction was stopped with 125 mM glycine. The ChIP assay with GFP Antibody (B-2) (Santa Cruz Biotechnology, sc-9996) and Protein A/G PLUS-Agarose (Santa Cruz Biotechnology, sc-2003) was performed following the protocol previously described (Gendrel et al., 2005), but with modifications at the Chelex resin-based DNA extraction step. Briefly, the washed beads, as well as the input samples, were incubated with 0.2 mL 10% Chelex-100 resin (Bio-Rad, #1421253) at 100°C for 10 min. After cooling down, 4 μg Proteinase K (New England Biolabs, P8107S) was added to the mix, followed by incubation at 50°C for 1 h. Proteinase K was then inactivated by heating at 100°C for 10 min. The supernatant of each tube was harvested by centrifuging at 4000×***g*** for 10 min. The supernatant was diluted and then interrogated with gene-specific primers and SsoAdvanced Universal SYBR® Green Supermix (Bio-Rad, #1725274) for qPCR reactions in 96-well blocks with the CFX Connect Real-Time PCR Detection System (Bio-Rad). Percent Input calculated from the qPCR Ct values was used to describe the enrichment of DNA fragments. The sequences of relevant primers are listed in Table S1.

Recombinant protein expression and purification

Sequences encoding mCherry and ELF3-Prd (residues 388-625) were sequentially subcloned into *pMAL-c6T vector* (New England Biolabs, N0378S) using the EcoRI and HindIII, BamHI, and EcoRI sites to generate *pMAL-ELF3-Prd-mCherry-c6T* vector. The vector was transformed into BL21-CodonPlus (DE3)-RIPL competent cells (Agilent, #230280). Recombinant protein was expressed and purified according to the instruction manual of NEBExpress® MBP Fusion and Purification System (New England Biolabs, #E8201S).

Liquid droplet formation with or without SA

The buffer of eluted MBP-ELF3-Prd-mCherry protein was changed to 20 mM Tris pH 8.0, 200 mM NaCl, and 1 mM TCEP using Vivaspin® 500 Centrifugal Concentrator (Sartorius, VS0122). About 0.5 μg μL^{-1} MBP-ELF3-Prd-mCherry protein was incubated with 1 mM SA as indicated, and 6% PEG4000 was then added to trigger LLPS of the protein. Droplets on the glass slide were imaged using confocal laser scanning microscopy.

Confocal laser scanning microscopy

Fluorescence imaging was done with Olympus FluoView FV3000 Inverted. For plant fluorescence microscopy, seedlings of *pELF3:ELF3-mGFP* in each genotype background were incubated at 29°C for 3 h. Roots from indicated plants were imaged by confocal microscopy with a 60×/1.42 oil Olympus UPlanXApo objective lens. GFP was excited at 488 nm excitation laser, and emission was detected at 510 nm. For visualization of MBP-ELF3-Prd-mCherry liquid droplets, images were acquired by confocal microscopy with a 20×/0.75 dry Olympus UPlanXApo objective lens. mCherry was excited at 587 nm excitation laser, and emission was detected at 610 nm. Identical acquisition parameters, including excitation laser intensity, emission light range, and exposure settings, were used for all images within each experiment.

GUS staining assay

Seedlings were sampled and soaked in GUS staining solution (0.1 M phosphate buffer, pH = 7.0, 0.1% Triton X-100, 0.5 mM $K_3(Fe[CN]_6)$, 0.5 mM $K_4(Fe[CN]_6)$, 10 mM EDTA, 0.5 mg mL^{-1} X-Gluc (5-bromo-4-chloro-3-indolyl-β-D-glucuronic acid)) at 37°C for 4 h in darkness. After being transferred to 75% ethanol for decolorization, seedlings were imaged with a color wide field upright microscope (Zeiss).

ACKNOWLEDGMENTS

This work was supported by Disruptive & Sustainable Technologies for Agricultural Precision (DiSTAP) research program, which is funded by the National Research Foundation (NRF), Singapore, under its campus for Research Excellence and Technological Enterprise (CREATE) program.

AUTHOR CONTRIBUTIONS

XC and N-HC designed the experiments. XC, YL, MRBJ, and JMS performed the experiments. XC, YL, RS, and N-HC analyzed the data. XC and N-HC wrote the manuscript.

CONFLICT OF INTEREST

The authors declare no conflict of interest.

DATA AVAILABILITY STATEMENT

All the data presented in this study are available in the manuscript and supporting information.

SUPPORTING INFORMATION

Additional Supporting Information may be found in the online version of this article.

Figure S1. Suppression of thermomorphogenesis by various concentrations of exogenous SA.

Figure S2. Relative expression of *PR1* in WT seedlings in response to MeSA in the presence or absence of MeSA esterase inhibitor.

Figure S3. Application of SA reverses the enhanced thermomorphogenesis phenotype of *ics1* mutant.

Figure S4. PIF4-HA protein degradation rate in *35S:PIF4-HA* plants with or without SA treatment at warm temperature.

Figure S5. Effects of SA on ELF3 protein abundance.

Figure S6. MBP-ELF3-Prd-mCherry protein undergoes LLPS induced by PEG4000.

Table S1. List of primers used in this study.

REFERENCES

Ang, M.C., Saju, J.M., Porter, T.K., Mohaideen, S., Sarangapani, S., Khong, D.T. *et al.* (2024) Decoding early stress signaling waves in living plants using nanosensor multiplexing. *Nature Communications*, **15**, 2943.

Bellstaedt, J., Trenner, J., Lippmann, R., Poeschl, Y., Zhang, X., Friml, J. *et al.* (2019) A Mobile auxin signal connects temperature sensing in cotyledons with growth responses in hypocotyls. *Plant Physiology*, **180**, 757–766.

Box, M.S., **Huang, B.E.**, **Domijan, M.**, **Jaeger, K.E.**, **Khattak, A.K.**, **Yoo, S.J.** ***et al.*** (2015) ELF3 controls thermoresponsive growth in Arabidopsis. *Current Biology*, **25**, 194–199.

Casal, J.J. & **Balasubramanian, S.** (2019) Thermomorphogenesis. *Annual Review of Plant Biology*, **70**, 321–346.

Delker, C., **Quint, M.** & **Wigge, P.A.** (2022) Recent advances in understanding thermomorphogenesis signaling. *Current Opinion in Plant Biology*, **68**, 102231.

Ding, Y., **Sun, T.**, **Ao, K.**, **Peng, Y.**, **Zhang, Y.**, **Li, X.** ***et al.*** (2018) Opposite roles of salicylic acid receptors NPR1 and NPR3/NPR4 in transcriptional regulation of plant immunity. *Cell*, **173**, 1454–1467.e1415.

Emoto, A., **Ushigome, F.**, **Koyabu, N.**, **Kajiya, H.**, **Okabe, K.**, **Satoh, S.** ***et al.*** (2002) H(+)-linked transport of salicylic acid, an NSAID, in the human trophoblast cell line BeWo. *American Journal of Physiology. Cell Physiology*, **282**, C1064–C1075.

Ezer, D., **Jung, J.H.**, **Lan, H.**, **Biswas, S.**, **Gregoire, L.**, **Box, M.S.** ***et al.*** (2017) The evening complex coordinates environmental and endogenous signals in Arabidopsis. *Nature Plants*, **3**, 17087.

Franklin, K.A., **Lee, S.H.**, **Patel, D.**, **Kumar, S.V.**, **Spartz, A.K.**, **Gu, C.** ***et al.*** (2011) Phytochrome-interacting factor 4 (PIF4) regulates auxin biosynthesis at high temperature. *Proceedings of the National Academy of Sciences of the United States of America*, **108**, 20231–20235.

Fu, Z.Q., **Yan, S.**, **Saleh, A.**, **Wang, W.**, **Ruble, J.**, **Oka, N.** ***et al.*** (2012) NPR3 and NPR4 are receptors for the immune signal salicylic acid in plants. *Nature*, **486**, 228–232.

Gendrel, A.V., **Lippman, Z.**, **Martienssen, R.** & **Colot, V.** (2005) Profiling histone modification patterns in plants using genomic tiling microarrays. *Nature Methods*, **2**, 213–218.

Gray, W.M., **Ostin, A.**, **Sandberg, G.**, **Romano, C.P.** & **Estelle, M.** (1998) High temperature promotes auxin-mediated hypocotyl elongation in Arabidopsis. *Proceedings of the National Academy of Sciences of the United States of America*, **95**, 7197–7202.

Huang, W., **Wang, Y.**, **Li, X.** & **Zhang, Y.** (2020) Biosynthesis and regulation of salicylic acid and N-hydroxypipecolic acid in plant immunity. *Molecular Plant*, **13**, 31–41.

Hutin, S., **Kumita, J.R.**, **Strotmann, V.I.**, **Dolata, A.**, **Ling, W.L.**, **Louafi, N.** ***et al.*** (2023) Phase separation and molecular ordering of the prion-like domain of the Arabidopsis thermosensory protein EARLY FLOWERING 3. *Proceedings of the National Academy of Sciences of the United States of America*, **120**, e2304714120.

Iglesias, M.J., **Terrile, M.C.** & **Casalongué, C.A.** (2011) Auxin and salicylic acid signalings counteract the regulation of adaptive responses to stress. *Plant Signaling & Behavior*, **6**, 452–454.

Jia, X., **Xu, Z.**, **Xu, L.**, **Frene, J.P.**, **Gonin, M.**, **Wang, L.** ***et al.*** (2025) Identification of new salicylic acid signaling regulators for root development and microbiota composition in plants. *Journal of Integrative Plant Biology*, **67**, 345–354.

Jung, J.H., **Barbosa, A.D.**, **Hutin, S.**, **Kumita, J.R.**, **Gao, M.**, **Derwort, D.** ***et al.*** (2020) A prion-like domain in ELF3 functions as a thermosensor in Arabidopsis. *Nature*, **585**, 256–260.

Jung, J.H., **Domijan, M.**, **Klose, C.**, **Biswas, S.**, **Ezer, D.**, **Gao, M.** ***et al.*** (2016) Phytochromes function as thermosensors in Arabidopsis. *Science*, **354**, 886–889.

Kaya, C., **Ugurlar, F.**, **Ashraf, M.** & **Ahmad, P.** (2023) Salicylic acid interacts with other plant growth regulators and signal molecules in response to stressful environments in plants. *Plant Physiology and Biochemistry*, **196**, 431–443.

Ke, M., **Ma, Z.**, **Wang, D.**, **Sun, Y.**, **Wen, C.**, **Huang, D.** ***et al.*** (2021) Salicylic acid regulates PIN2 auxin transporter hyperclustering and root gravitropic growth via Remorin-dependent lipid nanodomain organisation in *Arabidopsis thaliana*. *The New Phytologist*, **229**, 963–978.

Kim, J.H., **Castroverde, C.D.M.**, **Huang, S.**, **Li, C.**, **Hilleary, R.**, **Seroka, A.** ***et al.*** (2022) Increasing the resilience of plant immunity to a warming climate. *Nature*, **607**, 339–344.

Koini, M.A., **Alvey, L.**, **Allen, T.**, **Tilley, C.A.**, **Harberd, N.P.**, **Whitelam, G.C.** ***et al.*** (2009) High temperature-mediated adaptations in plant architecture require the bHLH transcription factor PIF4. *Current Biology*, **19**, 408–413.

Lai, Y.S., **Renna, L.**, **Yarema, J.**, **Ruberti, C.**, **He, S.Y.** & **Brandizzi, F.** (2018) Salicylic acid-independent role of NPR1 is required for protection from proteotoxic stress in the plant endoplasmic reticulum. *Proceedings of the National Academy of Sciences of the United States of America*, **115**, e5203–e5212.

Li, A., **Sun, X.** & **Liu, L.** (2022) Action of salicylic acid on plant growth. *Frontiers in Plant Science*, **13**, 878076.

Lorrain, S., **Allen, T.**, **Duek, P.D.**, **Whitelam, G.C.** & **Fankhauser, C.** (2008) Phytochrome-mediated inhibition of shade avoidance involves degradation of growth-promoting bHLH transcription factors. *The Plant Journal*, **53**, 312–323.

Lu, H.P., **Wang, J.J.**, **Wang, M.J.** & **Liu, J.X.** (2021) Roles of plant hormones in thermomorphogenesis. *Stress Biology*, **1**, 20.

Manohar, M., **Tian, M.**, **Moreau, M.**, **Park, S.W.**, **Choi, H.W.**, **Fei, Z.** ***et al.*** (2014) Identification of multiple salicylic acid-binding proteins using two high throughput screens. *Frontiers in Plant Science*, **5**, 777.

Maruri-Lopez, I. & **Chodasiewicz, M.** (2023) Involvement of small molecules and metabolites in regulation of biomolecular condensate properties. *Current Opinion in Plant Biology*, **74**, 102385.

Mizuno, T., **Nomoto, Y.**, **Oka, H.**, **Kitayama, M.**, **Takeuchi, A.**, **Tsubouchi, M.** ***et al.*** (2014) Ambient temperature signal feeds into the circadian clock transcriptional circuitry through the EC night-time repressor in *Arabidopsis thaliana*. *Plant & Cell Physiology*, **55**, 958–976.

Murcia, G., **Nieto, C.**, **Sellaro, R.**, **Prat, S.** & **Casal, J.J.** (2022) Hysteresis in PHYTOCHROME-INTERACTING FACTOR 4 and EARLY-FLOWERING 3 dynamics dominates warm daytime memory in Arabidopsis. *Plant Cell*, **34**, 2188–2204.

Nusinow, D.A., **Helfer, A.**, **Hamilton, E.E.**, **King, J.J.**, **Imaizumi, T.**, **Schultz, T.F.** ***et al.*** (2011) The ELF4-ELF3-LUX complex links the circadian clock to diurnal control of hypocotyl growth. *Nature*, **475**, 398–402.

Olate, E., **Jiménez-Gómez, J.M.**, **Holuigue, L.** & **Salinas, J.** (2018) NPR1 mediates a novel regulatory pathway in cold acclimation by interacting with HSFA1 factors. *Nature Plants*, **4**, 811–823.

Park, S.W., **Liu, P.P.**, **Forouhar, F.**, **Vlot, A.C.**, **Tong, L.**, **Tietjen, K.** ***et al.*** (2009) Use of a synthetic salicylic acid analog to investigate the roles of methyl salicylate and its esterases in plant disease resistance. *The Journal of Biological Chemistry*, **284**, 7307–7317.

Pasternak, T., **Groot, E.P.**, **Kazantsev, F.V.**, **Teale, W.**, **Omelyanchuk, N.**, **Kovrizhnykh, V.** ***et al.*** (2019) Salicylic acid affects root meristem patterning via auxin distribution in a concentration-dependent manner. *Plant Physiology*, **180**, 1725–1739.

Peng, Y., **Yang, J.**, **Li, X.** & **Zhang, Y.** (2021) Salicylic acid: biosynthesis and signaling. *Annual Review of Plant Biology*, **72**, 761–791.

Pokotylo, I., **Hodges, M.**, **Kravets, V.** & **Ruelland, E.** (2022) A ménage à trois: salicylic acid, growth inhibition, and immunity. *Trends in Plant Science*, **27**, 460–471.

Pokotylo, I., **Kravets, V.** & **Ruelland, E.** (2019) Salicylic acid binding proteins (SABPs): the hidden forefront of salicylic acid Signalling. *International Journal of Molecular Sciences*, **20**, 4377.

Press, M.O., **Lanctot, A.** & **Queitsch, C.** (2016) PIF4 and ELF3 act independently in *Arabidopsis thaliana* thermoresponsive flowering. *PLoS One*, **11**, e0161791.

Qi, G., **Chen, J.**, **Chang, M.**, **Chen, H.**, **Hall, K.**, **Korin, J.** ***et al.*** (2018) Pandemonium breaks out: disruption of salicylic acid-mediated defense by plant pathogens. *Molecular Plant*, **11**, 1427–1439.

Quint, M., **Delker, C.**, **Balasubramanian, S.**, **Balcerowicz, M.**, **Casal, J.J.**, **Castroverde, C.D.M.** ***et al.*** (2023) 25 years of thermomorphogenesis research: milestones and perspectives. *Trends in Plant Science*, **28**, 1098–1100.

Raschke, A., **Ibañez, C.**, **Ullrich, K.K.**, **Anwer, M.U.**, **Becker, S.**, **Glöckner, A.** ***et al.*** (2015) Natural variants of ELF3 affect thermomorphogenesis by transcriptionally modulating PIF4-dependent auxin response genes. *BMC Plant Biology*, **15**, 197.

Rekhter, D., **Lüdke, D.**, **Ding, Y.**, **Feussner, K.**, **Zienkiewicz, K.**, **Lipka, V.** ***et al.*** (2019) Isochorismate-derived biosynthesis of the plant stress hormone salicylic acid. *Science*, **365**, 498–502.

Rivas-San Vicente, M. & **Plasencia, J.** (2011) Salicylic acid beyond defence: its role in plant growth and development. *Journal of Experimental Botany*, **62**, 3321–3338.

Rong, D., **Luo, N.**, **Mollet, J.C.**, **Liu, X.** & **Yang, Z.** (2016) Salicylic acid regulates pollen tip growth through an NPR3/NPR4-independent pathway. *Molecular Plant*, **9**, 1478–1491.

Stavang, J.A., **Gallego-Bartolomé, J.**, **Gómez, M.D.**, **Yoshida, S.**, **Asami, T.**, **Olsen, J.E.** ***et al.*** (2009) Hormonal regulation of temperature-induced growth in Arabidopsis. *The Plant Journal*, **60**, 589–601.

Sun, J., **Qi, L.**, **Li, Y.**, **Chu, J.** & **Li, C.** (2012) PIF4-mediated activation of YUCCA8 expression integrates temperature into the auxin pathway in regulating arabidopsis hypocotyl growth. *PLoS Genetics*, **8**, e1002594.

Tan, S., **Abas, M.**, **Verstraeten, I.**, **Glanc, M.**, **Molnár, G.**, **Hajný, J.** ***et al.*** (2020) Salicylic acid targets protein phosphatase 2A to attenuate growth in plants. *Current Biology*, **30**, 381–395.e388.

Torrens-Spence, M.P., **Bobokalonova, A.**, **Carballo, V.**, **Glinkerman, C.M.**, **Pluskal, T.**, **Shen, A.** ***et al.*** (2019) PBS3 and EPS1 complete salicylic acid biosynthesis from isochorismate in Arabidopsis. *Molecular Plant*, **12**, 1577–1586.

Tripathi, D., **Jiang, Y.L.** & **Kumar, D.** (2010) SABP2, a methyl salicylate esterase is required for the systemic acquired resistance induced by acibenzolar-S-methyl in plants. *FEBS Letters*, **584**, 3458–3463.

Undurraga, S.F., **Press, M.O.**, **Legendre, M.**, **Bujdoso, N.**, **Bale, J.**, **Wang, H.** ***et al.*** (2012) Background-dependent effects of polyglutamine variation in the *Arabidopsis thaliana* gene ELF3. *Proceedings of the National Academy of Sciences of the United States of America*, **109**, 19363–19367.

van Butselaar, T., **Silva, S.**, **Lapin, D.**, **Bañales, I.**, **Tonn, S.**, **van Schie, C.** ***et al.*** (2024) The role of salicylic acid in the expression of RECEPTOR-LIKE PROTEIN 23 and other immunity-related genes. *Phytopathology*, **114**, 1097–1105.

Vu, L.D., **Xu, X.**, **Gevaert, K.** & **De Smet, I.** (2019) Developmental plasticity at high temperature. *Plant Physiology*, **181**, 399–411.

Wang, D., **Pajerowska-Mukhtar, K.**, **Culler, A.H.** & **Dong, X.** (2007) Salicylic acid inhibits pathogen growth in plants through repression of the auxin signaling pathway. *Current Biology*, **17**, 1784–1790.

Wang, X., **Zhao, C.**, **Müller, C.**, **Wang, C.**, **Ciais, P.**, **Janssens, I.** ***et al.*** (2020) Emergent constraint on crop yield response to warmer temperature from field experiments. *Nature Sustainability*, **3**, 908–916.

Wildermuth, M.C., **Dewdney, J.**, **Wu, G.** & **Ausubel, F.M.** (2001) Isochorismate synthase is required to synthesize salicylic acid for plant defence. *Nature*, **414**, 562–565.

Wu, Y., **Zhang, D.**, **Chu, J.Y.**, **Boyle, P.**, **Wang, Y.**, **Brindle, I.D.** ***et al.*** (2012) The Arabidopsis NPR1 protein is a receptor for the plant defense hormone salicylic acid. *Cell Reports*, **1**, 639–647.

Yuan, H.M., **Liu, W.C.** & **Lu, Y.T.** (2017) CATALASE2 coordinates SA-mediated repression of both auxin accumulation and JA biosynthesis in plant defenses. *Cell Host & Microbe*, **21**, 143–155.

Zhang, L.L., **Shao, Y.J.**, **Ding, L.**, **Wang, M.J.**, **Davis, S.J.** & **Liu, J.X.** (2021) XBAT31 regulates thermoresponsive hypocotyl growth through mediating degradation of the thermosensor ELF3 in Arabidopsis. *Science Advances*, **7**, eabf4427.

Zhang, X., **Henriques, R.**, **Lin, S.S.**, **Niu, Q.W.** & **Chua, N.H.** (2006) Agrobacterium-mediated transformation of *Arabidopsis thaliana* using the floral dip method. *Nature Protocols*, **1**, 641–646.

Zhang, Y., **Zhao, L.**, **Zhao, J.**, **Li, Y.**, **Wang, J.**, **Guo, R.** ***et al.*** (2017) S5H/DMR6 encodes a salicylic acid 5-hydroxylase that fine-tunes salicylic acid homeostasis. *Plant Physiology*, **175**, 1082–1093.

Zhang, Z., **Li, Q.**, **Li, Z.**, **Staswick, P.E.**, **Wang, M.**, **Zhu, Y.** ***et al.*** (2007) Dual regulation role of GH3.5 in salicylic acid and auxin signaling during Arabidopsis-pseudomonas syringae interaction. *Plant Physiology*, **145**, 450–464.

Zhu, P., **Burney, J.**, **Chang, J.**, **Jin, Z.**, **Mueller, N.D.**, **Xin, Q.** ***et al.*** (2022) Warming reduces global agricultural production by decreasing cropping frequency and yields. *Nature Climate Change*, **12**, 1016–1023.

Zhu, Z., **Trenner, J.**, **Delker, C.** & **Quint, M.** (2024) Tracing the evolutionary history of the temperature-sensing prion-like domain in EARLY FLOWERING 3 highlights the uniqueness of AtELF3. *Molecular Biology and Evolution*, **41**, msae205.

Zuo, J., **Niu, Q.W.** & **Chua, N.H.** (2000) Technical advance: an estrogen receptor-based transactivator XVE mediates highly inducible gene expression in transgenic plants. *Plant Journal*, **24**, 265–273.